ResearchGate

See discussions, stats, and author profiles for this publication at: https://www.researchgate.net/publication/259369345

Temperature Dependence of Looping Rates in a Short Peptide

ARTICLE *in* THE JOURNAL OF PHYSICAL CHEMISTRY B · FEBRUARY 2007

Impact Factor: 3.3

CITATIONS
3

READS
21

4 AUTHORS, INCLUDING:

Danilo Roccatano
University of Lincoln
103 PUBLICATIONS **2,326** CITATIONS
SEE PROFILE

Harekrushna Sahoo
National Institute of Technology Rourkela
14 PUBLICATIONS **84** CITATIONS
SEE PROFILE

Werner M Nau
Jacobs University
307 PUBLICATIONS **7,376** CITATIONS
SEE PROFILE

Available from: Harekrushna Sahoo
Retrieved on: 26 January 2016

Temperature Dependence of Looping Rates in a Short Peptide

Danilo Roccatano,* Harekrushna Sahoo, Martin Zacharias, and Werner M. Nau*

School of Engineering and Science, Jacobs University of Bremen, Campus Ring 1, D-28759, Bremen, Germany

Received: September 29, 2006; In Final Form: January 15, 2007

Knowledge of the influence of chain length and amino acid sequence on the structural and dynamic properties of small peptides in solution provides essential information on protein folding pathways. The combination of time-resolved optical spectroscopy and molecular dynamics (MD) simulation methods has become a powerful tool to investigate the kinetics of end-to-end collisions (looping rates) in short peptides, which are relevant in early protein folding events. We applied the combination of both techniques to study temperature-dependent (280−340 K) looping rates of the Dbo-AlaGlyGln-Trp-NH_2 peptide, where Dbo represents a 2,3-diazabicyclo-[2.2.2]oct-2-ene-labeled asparagine, which served as a fluorescent probe in the time-resolved spectroscopic experiments. The experimental looping rates increased from 4.8×10^7 s^{-1} at 283 K to 2.0×10^8 s^{-1} at 338 K in H_2O. The corresponding Arrhenius plot provided as activation parameters $E_a = 21.5 \pm 1.0$ kJ mol^{-1} and $\ln(A/s^{-1}) = 26.8 \pm 0.2$ in H_2O. The results in D_2O were consistent with a slight solvent viscosity effect, i.e., the looping rates were 10−20% slower. MD simulations were performed with the GROMOS96 force field in a water solvent model, which required first a parametrization of the synthetic amino acid Dbo. After corrections for solvent viscosity effects, the calculated looping rates varied from 1.5×10^8 s^{-1} at 280 K to 8.2×10^8 s^{-1} at 340 K in H_2O, which was about four times larger than the experimental data. The calculated activation parameters were $E_a = 24.7 \pm 1.5$ kJ mol^{-1} and $\ln(A/s^{-1}) = 29.4 \pm 0.1$ in H_2O.

Introduction

The understanding of the dynamic behavior of peptides in solution is a prerequisite for deciphering the protein folding process. The elementary rates by which different regions of peptides form intrachain contacts limit the formation of secondary and tertiary structural motifs, in particular hairpins and loops. Several methodologies based on nanosecond time-resolved optical spectroscopy have recently emerged[1−14] to allow direct measurement of the kinetics of end-to-end collision (looping rates) in short peptides. Our fluorescence-based technique, for example, involves the intramolecular quenching of a 2,3-diazabicyclo[2.2.2]oct-2-ene-labeled asparagine (Dbo) by Trp to measure the looping rates.[9−12] The resulting looping rate constants range typically from 10^8 to 10^6 s^{-1}. This provides an ideal range for comparison with state-of-the art molecular dynamics (MD) simulations, which allows one to furnish an understanding of the process in atomistic detail.[15,16] The previous comparisons of experimental data and MD simulation results have focused on looping rate constants in dependence on the employed force field and the required corrections for experimental as well as computational deviations.[15,16] In particular, some experimental systems afford looping rates that are systematically too small due to insufficiently efficient quenching,[1−4] and the MD simulations afford rates that are too fast as a consequence of the choice of a particular force field and the lower-than-experimental viscosity of the solvent model.[17]

Herein, we investigate how well MD simulations are capable of reproducing the temperature dependence of looping kinetics by using the GROMOS96 force field.[18] As an experimental model, we have returned to the AlaGlyGln backbone originally introduced by Lapidus et al.,[1−3] who employed Trp as a probe and Cys as a quencher (Cys-AlaGlyGln-Trp). For the present study, the peptide was appropriately modified (Dbo-AlaGlyGln-Trp-NH_2) to allow the introduction of Dbo as fluorescent probe. As was demonstrated in previous studies,[9−12] the fluorescence quenching rates in the Dbo/Trp probe/quencher system provide a direct measure of the looping rates and can be conveniently and accurately investigated in dependence on temperature.[11,12] GROMOS96 parameters for the synthetic amino acid Dbo were implemented to perform the temperature-dependent MD simulations of the looping rates. To the best of our knowledge, this is the first study employing MD methods to simulate the temperature dependence of experimentally accessible dynamic properties of a short peptide.

Materials and Methods

Time-Resolved Spectroscopic Measurements. The probe/quencher containing peptide, Dbo-AlaGlyGln-Trp-NH_2, was commercially synthesized with a purity >95% (Biosyntan, Berlin). Details on the synthesis of the probe and its suitability in solid-phase peptide synthesis have been reported.[10] D_2O was used as received from Applichem (99.8 %D). Nanopure water (PURELAB) was used.

The fluorescence decays of the peptide (ca. 50 μM) were measured in D_2O and H_2O under air at temperatures ranging from 338 to 340 K by time-correlated single-photon counting (FLS920, Edinburgh Instruments Ltd.) by using a PicoQuant diode laser LDH-P-C 375 ($\lambda_{exc} = 373$ nm, $\lambda_{obs} = 450$ nm, fwhm ca. 50 ps) as the excitation source. The temperature in the cuvette was controlled with a circulating water bath (Julabo F25/HD thermostat) through a feedback loop with the temperature probe placed directly inside the cuvette to precisely maintain the target temperature within ±0.1 °C. Errors in experimental lifetimes

* E-mail: d.roccatano@iu-bremen.de (D.R.); w.nau@iu-bremen.de (W.M.N.).

10.1021/jp066418m CCC: $37.00 © 2007 American Chemical Society
Published on Web 02/16/2007

SCHEME 1: Molecular Structures of the Synthetic Amino Acid Dbo and the Investigated Peptide, Dbo-AlaGlyGln-Trp-NH_2

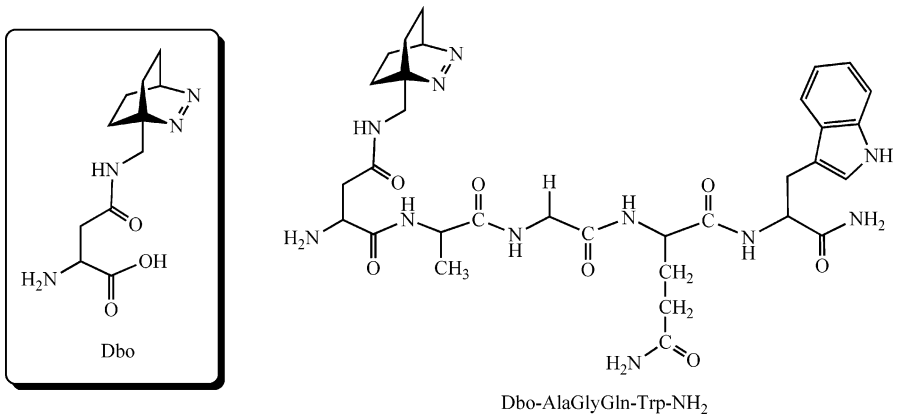

SCHEME 2: Definition of Dihedral Angles

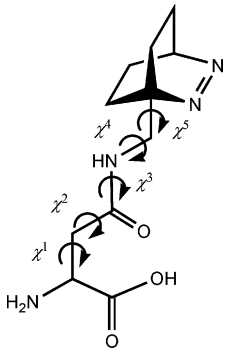

are reported as standard deviations obtained from the reconvolution fitting implemented in the instrument-specific software. The errors in the rate constants (10%) are reported as triple standard deviations.

Dbo Amino Acid Parametrization. A minimalist approach to the parametrization of the synthetic amino acid Dbo was adopted. Where possible, parameters already available in the GROMOS96 force field[18] were used (for asparagine). In particular, van der Waals parameters and partial atomic charges were assigned according to atom types present in the GROMOS96 force field, and all the aliphatic carbon atoms were considered as united atoms. The conformational analysis of the peptide revealed three dominant conformers, which differed with respect to the trans and cis amide bond stereochemistry (angle χ^3 in Scheme 2; see Table S1 in the Supporting Information). The amino acid conformer with the lowest energy (Figure 1) was used to calculate the partial atomic charges by fitting (using the CHELPG method)[19] the molecular-mechanics-derived electrostatic potential to that obtained from quantum-chemical calculations (ab initio restricted HF 6-31+G*, using the Gaussian 03 software package).[20] These partial charges were averaged with those obtained from the symmetry-related minimum energy conformation to afford the values reported in Table S2 of the Supporting Information. Note that the difference in dipole moments of the 2,3-diazabicyclo[2.2.2.]oct-2-ene chromophore in its ground- and excited-state is small,[21] such that no corrections for redistribution of charges due to excitation were made, i.e., we assume that the electronic excitation does not alter the structural and dynamic properties of the peptide, in keeping with the common procedure in MD simulations for other optical probes.[16]

Because united atoms were used for the aliphatic carbons, the torsion parameters on the χ^4 and χ^5 dihedrals (see Scheme 2) were modeled to obtain (i) a distribution of angles co-incident with the quantum-mechanically optimized minima and (ii) relative conformer populations in qualitative agreement with the relative energy of the different minima. The parameters for the χ^1 and χ^2 dihedrals were taken to be the same of those for the asparagine residue.

Equilibrium values for bond lengths, bond angles, and dihedrals were also estimated from the quantum-mechanically calculated ground-state geometry. Force constants were obtained from the GROMOS96 force field library, where available, otherwise from the OPLS force field[22,23] parameter set. The new force field parameters established for the synthetic amino acid Dbo are reported in Table S3 of the Supporting Information. The starting structure of Dbo was subsequently minimized in vacuum using the new force field (see Figure 1); the conformation of the side chain in the resulting MD-optimized structure closely resembled the quantum-mechanically optimized one.

Molecular Dynamics Simulations. The MD runs and the analysis of the trajectories were performed using the GROMACS software package,[24,25] and all cutoff values were kept the same as those used for the original force field parametrization.[18] The detailed simulations were performed according to the previously established protocol for use of the GROMOS96 force field to calculate looping dynamics,[15] except that the peptide was simulated at six different temperatures (280,

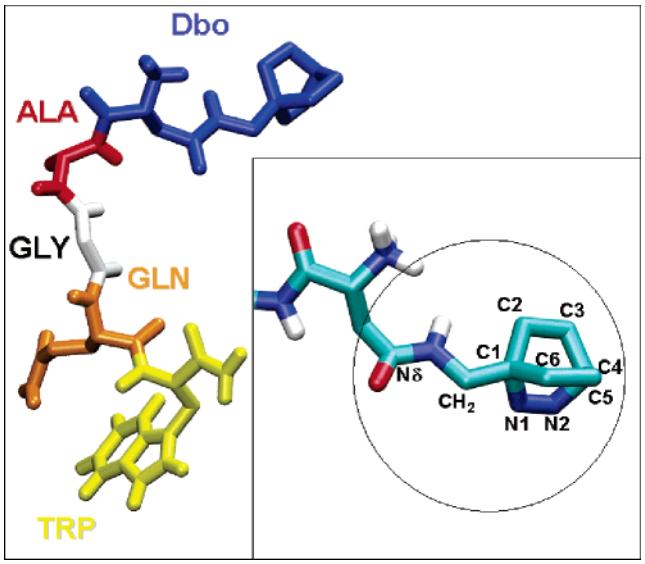

Figure 1. The Dbo-AlaGlyGln-Trp-NH_2 peptide in an extended configuration. In the inset, the nomenclature for the parametrization of the synthetic amino acid Dbo is specified.

290, 300, 310, 325, 340 K) and that the production runs, after the equilibration, were consistently performed for 100 ns. The starting structure of the peptide was modeled in an extended conformation, with the C terminus amidated and the N-terminal amino group protonated to match the experimental conditions (pH ca. 7). The peptide was solvated with water molecules in sufficiently large periodic cubic boxes to contain the molecule and 0.9 nm of solvent on all sides. All solvent molecules within 0.15 nm of any amino acid atom were removed. Because the resulting protonation state of the peptide gives a total charge of +1 (due to the N-terminal ammonium group), one chloride counterion was added by replacing a water molecule at the most negative electrical potential to provide a neutral simulation box. As was shown in a previous paper,[15] the improvements resulting from the use of the Particle Mesh Ewalds method are expected to be minor, which did not justify the required extra computational time.

Shear Viscosity. Shear viscosities were calculated at 280, 300, and 340 K using the method described by Hess,[26] which is implemented in GROMACS.[24,25] In this method, the viscosity of the liquid is estimated from nonequilibrium simulations. i.e., an external shear-stress acceleration field is applied to the system:

$$a_{i,x} = A\cos\left(\frac{2\pi Z_i}{l_Z}\right) \tag{1}$$

$a_{i,x}$ is the acceleration in the x direction, A is the acceleration amplitude, Z_i is the z-coordinate of the particle, and l_Z is the length of the box in the z-direction. The external acceleration field induces a velocity gradient of the same shape. Under these conditions, for a classical (Newtonian) fluid, the dynamic viscosity (η) is simply given by

$$\eta = \frac{A}{\upsilon}\sigma\left(\frac{l_Z}{2\pi}\right)^2 \tag{2}$$

where σ is the density of the system and υ is the resulting velocity amplitude. A careful choice of the A parameter as well as of the box edge in the z-direction[26] was made in order to induce a perturbation to the system that was discernible from thermal velocities but still small enough to prevent the appearance of order in the fluid. A rectangular box of 3.74 × 3.74 × 7.47 nm and a value for A of 0.025, 0.025, and 0.015 nm ps^{-2} were used for the 280, 300, and 340 K simulations, respectively.

Cluster Analysis and Kinetic Analysis of the Looping Rates. The cluster analysis of trajectories was performed by using the method proposed by Daura et al.[27] on conformations sampled every 50 ps. The clustering algorithm was applied to all heavy atoms of the peptide. The criteria of similarity for two structures was a positional root-mean-square deviation.[28] A cutoff of 0.25 nm was used. The looping rates (rate constants for end-to-end collision) were extracted from the MD simulated data according to our previously established protocol.[15] In order to define cutoff values for a contact distance between Dbo and Trp, i.e., to define conformations as collision complexes, the contact distance (R) between the bicyclic chromophore and the indole ring was calculated with respect to the middle of the central C−C bond of the indole ring and the central point of the N═N bond (Scheme 3), because electronic excitation in Dbo is localized on the azo group,[29] and quenching occurs presumably by interaction of the azo group with the aromatic π system.[11]

The diffusion-limited mean first contact passage time can be calculated from the distribution of the time intervals

SCHEME 3: Definition of the End-to-End Distance Parameter (*R*)

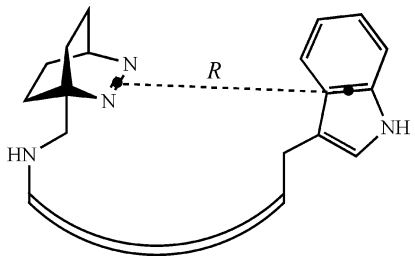

between contacts:[30,31]

$$\Delta_k = \{t_j - t_i | R(t_{i-1}) \le r; R(t_i) > r; R(t_j) \le r\} \tag{3}$$

for $i < j$, and $k = 1...n_{\text{int}}$. We used a value of $r = 0.45$ nm for the contact distance (sink radius). Taking the initial distribution to be every conformation with $R(t) > r$ affords the equilibrium distribution of contact times $P(\tau)$ with a mean contact time $\tau_{\text{sim}} = (<\Delta^2>_{\text{sim}})/2(<\Delta>_{\text{sim}})$, which corresponds to the mean time between the formation of two loop structures. The distribution of $P(\tau)$ is characterized by a strong non-exponential behavior at short times produced by the sharp edge of the Heavyside sink.[31] The mean contact times were ultimately converted to looping rates (see Results and Discussion), which could be further corrected by appropriate factors to account for the lower viscosity of the SPC model with respect to real water.[15−17]

Results and Discussion

The present study deals with the measurements of end-to-end collision rates (looping) in peptides of the general structure A-AlaGlyGln-Z, where A/Z are probe/quencher pairs suitable for investigation by time-resolved spectroscopy; by measuring the looping rates, the dynamic flexibility of the peptide backbone, i.e., AlaGlyGln, can be assessed and its propensity for looping can be probed. The first measurements were performed by Lapidus et al.,[1,2] with Trp as a triplet transient probe (Z = Trp) and Cys as quencher (A = Cys). The raw experimental rate constant amounted to 1.37 × 10^7 s^{-1},[1,16] which was further corrected by taking into account a lower-than-diffusion controlled quenching (factor of 2) to afford a looping rate of 2.7 × 10^7 s^{-1}.[1] Yeh and Hummer[16] performed extensive MD simulations on the same peptide (Cys-AlaGlyGln-Trp), by using the AMBER94[32] and CHARMM[33] force fields and obtained looping rates of ca. 7 × 10^8 s^{-1}. Using a scaling factor for the solvent viscosity (factor 2.87) and a complex correction for the non-diffusion-controlled quenching rate (factor 17−28), one finds that the resulting apparent rate constants return in reasonable agreement with the experimental data,[16] i.e., ca. 1.4 × 10^7 s^{-1} for AMBER and ca. 7.9 × 10^6 s^{-1} for CHARMM. Subsequently, we have extended the MD simulations on this peptide to GROMOS96 and OPLS-AA as alternative force fields[15] and obtained rate constants of ca. 2 × 10^9 s^{-1}, which were again too large when compared with the then available experimental estimates. The differences in rate constants obtained by the different force fields were related to the nature of the calculated free energy landscape of the peptides, because the fastest intrachain collision kinetics was found for the force field with the smallest barrier toward formation of compact structures. According to these results, we could classify the bias of the different force fields toward predicting too fast dynamics as follows: GROMOS96 > OPLS-AA/L > AMBER94 ≥ CHARMM.[15] The aim of the present study was (a) to obtain improved experimental looping rate constants by applying Dbo

TABLE 1: Fluorescence Lifetimes (τ) of the Dbo-AlaGlyGln-Trp-NH_2 Peptide, Fluorescence Lifetimes of the Quencher-Unlabeled Reference Peptide[a] (τ_0), and Calculated Looping Rates[b] (k_{loop}) in H_2O

T/K	τ/ns[c]	τ_0/ns[a,d]	$k_{loop}/(10^7\ sec^{-1})$[b,e]
283	19.9	397	4.8
288	17.1	374	5.6
293	15.2	354	6.3
298	13.2	337	7.3
303	11.2	322	8.6
308	9.7	311	10.0
313	8.5	301	11.4
318	7.5	290	13.1
323	6.9	282	14.2
328	6.0	277	16.3
333	5.3	274	18.4
338	4.9	272	20.3

[a] $(Gly)_6$-Dbo was used as reference peptide (without quencher). [b] Calculated as $k_{loop} = 1/\tau - 1/\tau_0$. [c] Error ± 3%. [d] Error ± 5 ns. [e] Error ± 10%.

as probe (A = Dbo) with Trp as quencher (Z = Trp) in H_2O and D_2O and (b) to study the temperature dependence (280−340 K) of looping rates, both experimentally and by MD simulations, to open an additional (independent of the absolute rates) means to compare experiment with theory.

Time-Resolved Spectroscopic Measurements. The choice of the Dbo/Trp probe/quencher pair instead of the originally employed Trp/Cys one was motivated by the following considerations:[9,10,12] (i) the intrachain collision of Dbo with Trp can be monitored by fluorescence, which allows one to obtain accurate quenching rate data and which facilitates temperature-dependent measurements; (ii) fluorescence quenching of Dbo by Trp is close to diffusion-controlled, such that the resulting quenching rates can be directly taken as looping rates, thereby bypassing the need of corrections for non-diffusion-controlled quenching. Intramolecular fluorescence quenching was investigated for the peptide Dbo-AlaGlyGln-Trp-NH_2 (Scheme 1); Dbo was placed at the N terminus, and Trp was left at the C terminus to allow a better comparison with the Cys-AlaGlyGln-Trp peptide.

The fluorescence decays were recorded by time-correlated single photon counting in H_2O and D_2O. The experimental raw data are contained in Table 1 for H_2O and in Table S4 of the Supporting Information for D_2O. The time-resolved fluorescence decays at different temperatures were found to be non-monoexponential, suggesting that the conformational averaging within the very short fluorescence lifetimes (5−20 ns) of this short peptide is incomplete. In fact, although monoexponential fitting of the transient decays is frequently satisfactory,[10] it is not *a priori* expected[15,34] and depends on the time resolution and the experimental accuracy. A biexponential fitting was satisfactory ($\chi^2 < 1.1$) to describe the fluorescence decays, and average fluorescence lifetimes (τ) were determined as $\tau = \alpha_1\tau_1 + \alpha_2\tau_2$, where τ_1 and τ_2 were the two fitted lifetimes and α_1 and α_2 were their preexponential factors (with $\alpha_1 + \alpha_2 = 1$). The fluorescence lifetimes of the probe-only labeled reference peptide (τ_0) were always monoexponential. The intramolecular quenching rate constants (k_{loop}) were obtained as $k_{loop} = 1/\tau - 1/\tau_0$. They provide a direct experimental measure, based on the interpretations and analyses of our previous studies,[9−13] of the looping rate in short peptides (Table 1 and Table S4). The τ_0 values are very long (20−70 times larger than τ) and also not strongly temperature-dependent, such that corrections due to the $1/\tau_0$ term are in fact very minor. Note that the longer τ_0 values in D_2O (Table S4) are due to a less efficient solvent-induced quenching;[35] the longer τ values in D_2O (as well as the 10−20% slower 10−20% k_{loop} values in D_2O) are attributed to the slightly higher viscosity of D_2O,[11] which slows diffusion and thereby reduces the looping rates slightly but systematically.

The absolute values of the looping rate constants are of prime interest, because these rates have been considered as the "speed limit of protein folding".[5,6] The experimental looping rate constant measured for the Dbo-AlaGlyGln-Trp-NH_2 peptide at 298 K in water amounts to $(7.3 \pm 0.7) \times 10^7\ s^{-1}$ and is therefore substantially faster than the rate of $1.37 \times 10^7\ s^{-1}$ observed for the Cys-AlaGlyGln-Trp peptide.[1,3,4,16,36] Because both measurements refer to the flexibility of the same backbone (AlaGlyGln), the quenching efficiency of probe and quencher must differ significantly and needs to be held responsible for the contrast in experimental rates. In fact, the Cys/Trp probe/quencher pair has been recognized as being not fully intramolecularly diffusion-controlled. However, even a correction factor of 2 suggested for this pair[1,2,4] does not bring the two data sets into an acceptable agreement, such that additional factors must be held responsible, which could also be related to the different types of amino acids (Dbo versus Cys). Be this as it may, there appears to be presently an agreement[5,7,10,12] that the looping in short peptides, in particular glycine-containing ones, can be as fast as 20 ns or faster, consistent with the present looping rates of the Dbo-AlaGlyGln-Trp-NH_2 peptide (Table 1).

As expected for an activation-controlled process, the looping rate constants increased with increasing temperature in both solvents, e.g., from $4.8 \times 10^7\ s^{-1}$ at 283 K to $2.0 \times 10^8\ s^{-1}$ at 338 K in H_2O. The Arrhenius plots in both solvents were strictly linear ($r = 0.999$, $n = 12$) in the investigated temperature range, such that the activation energies (E_a) and pre-exponential factors ($\ln A$) could be obtained by linear regression analysis. The values we obtained were $E_a = 21.5 \pm 1.0$ kJ mol^{-1} and $\ln(A/s^{-1}) = 26.8 \pm 0.2$ in H_2O and $E_a = 22.9 \pm 1.0$ kJ mol^{-1} and $\ln(A/s^{-1}) = 27.3 \pm 0.2$ in D_2O. As shown previously,[11,12] a marginally higher activation energy in D_2O (ca. 1 kJ mol^{-1}) is theoretically expected on the basis of its higher viscosity[11] but difficult to corroborate experimentally due to the error limits.

Molecular Dynamics Simulations. Long time-scale MD simulations (100 ns) were performed using the GROMOS96 force field. Although this force field is known to give the "fastest" intrachain dynamics (see above),[15] it is broadly used to simulate protein and peptide folding[37,38] and was therefore preferred in the present context. The MD simulations provide sets of structures (clusters), which can be interpreted with respect to their geometrical peculiarities (structural properties) and, in a second step, analyzed with respect to the peptide dynamics by selecting cutoff criteria to define the desired events. The geometries at which fluorescence quenching of Dbo by Trp occurs need therefore to be defined to allow one to set meaningful cutoff criteria for end-to-end collision. In the case of the indole ring and the 2,3-diazabicyclo[2.2.2]oct-2-ene chromophore, the quenching process is presumed to be initiated by the formation of a charge-transfer bond between the single occupied lone pair orbital of one excited azo nitrogen atom with the aromatic π system. The resulting exciplex[10,11] is presumably deactivated through a close-lying conical intersection, which has been characterized in detail for amines as electron donors.[21,39] On the basis of the presumed geometry of the exciplex, in which the distance between the aromatic π system and the azo group presents the key parameter responsible for quenching, the distance between the centers of the N═N bond and the inner C−C indole bond was selected as a critical distance parameter (R, Scheme 3); any conformation with an R value below a

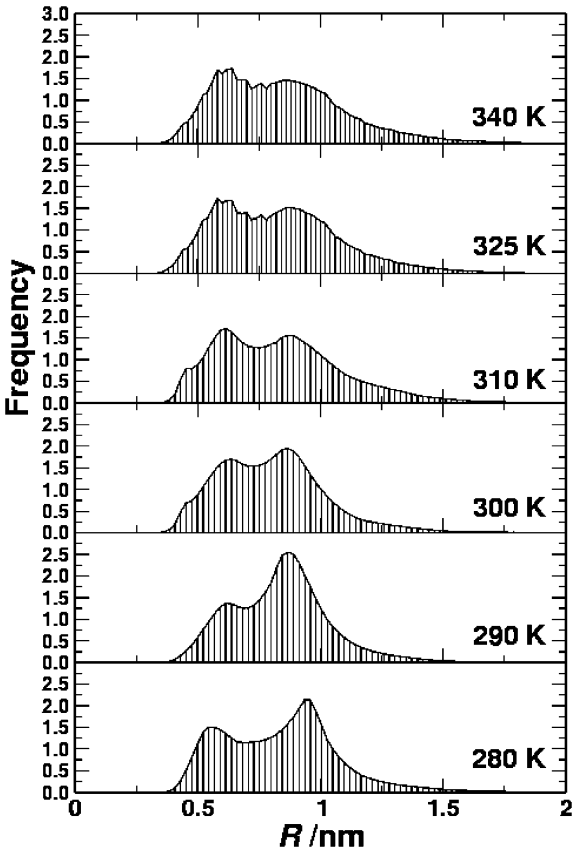

Figure 2. End-to-end distance distributions from the cumulative simulations at different temperatures.

critical distance of 4.5 Å, which was produced in the MD runs, was considered as a "hit", i.e., a successful quenching event.

The analysis of the structural properties was mainly conducted by focusing on the geometrical features relevant for the quenching process, namely on the end-to-end distance as defined by the probe/quencher distance R (see above). In Figure 2, the R distributions for the different simulations are reported. All curves are bimodal with two peaks at short and long distance, respectively. The position of the two peaks varies with temperature. At 280 K, the longer distance peak is located at 0.9 nm and the shorter one at 0.6 nm. At higher temperature, the two peaks become less separated, and in addition, the entire distribution becomes broader. The distinct short-distance peak at lower temperature can be related to a sizable contribution of a secondary structure motif (with a turn conformation at Gly3 or Gln4), which decreases systematically upon increasing the temperature (from 21% at 280 K to 2.5% at 340 K). The conformational nonuniformity (structured and random-coiled) borne out by the MD simulations could provide a viable explanation for the non-monoexponential fluorescence decays observed experimentally for the Dbo-AlaGlyGln-Trp-NH_2 peptide.

In order to understand the relation between the distribution of the end-to-end distance and the structure of the peptides, a cluster analysis was conducted on all trajectories. The first five clusters reported in Table 2 contain more than 50% of the analyzed conformations (8000 for each trajectory). The number of clusters increases, as expected, with temperature. In Figure 3, the average end-to-end distance for the first 20 clusters is reported for all simulations. The histogram in each panel indicates the percentage of conformations belonging to the cluster (see also Table 2). In Figure 4, the representative (median) structures of each of these clusters are reported. As

TABLE 2: Summary of the Cluster Analysis of the Simulations

T/K	# clusters	% 1	% 2	% 3	% 4	% 5	sum %
280	78	23.4	15.4	9.0	7.8	5.1	60.7
290	79	31.3	12.3	9.2	6.4	5.3	64.5
300	89	20.1	12.1	12.1	9.0	7.0	60.3
310	106	14.3	11.2	10.5	9.9	5.4	51.3
325	91	13.9	10.5	9.3	9.0	5.7	48.4
340	112	14.2	11.2	11.0	7.3	6.8	50.5

can be seen, the pictorial presentation of the different peptide conformations reveals a large flexibility of the peptide at the different temperatures. In most cases, the backbone conformation is bent, such that end-to-end contacts are facilitated by the side chain of the probe, which itself could be regarded as an extension of the peptide chain. The MD-calculated structures provide interesting information on how the looping between probe and quencher could occur in atomistic detail in this short peptide, thereby yielding information that is yet experimentally inaccessible.

Comparison of Experimental and Calculated Looping Kinetics. The analysis of the looping kinetics is reported in Table 3. The looping rate constants obtained by the MD simulations (k^{MD}) were calculated as $k^{MD} = 1/\tau_{sim}$, where the τ_{sim} values were the calculated mean contact times (see Materials and Methods). The theoretical rate constants were further corrected (k_{loop}^{MD}, Table 3) with a constant factor of 2.0 to account for the lower viscosity of the MD-simulated water model compared to the experimental viscosity of water.[15,16]

Comparison of the corrected MD-calculated data with the experimentally determined values (k_{loop}, Table 1) shows that the calculated rates are significantly faster than the experimentally observed ones, but the trend is very well reproduced and the difference is relatively constant (factor 4 ± 1, right column

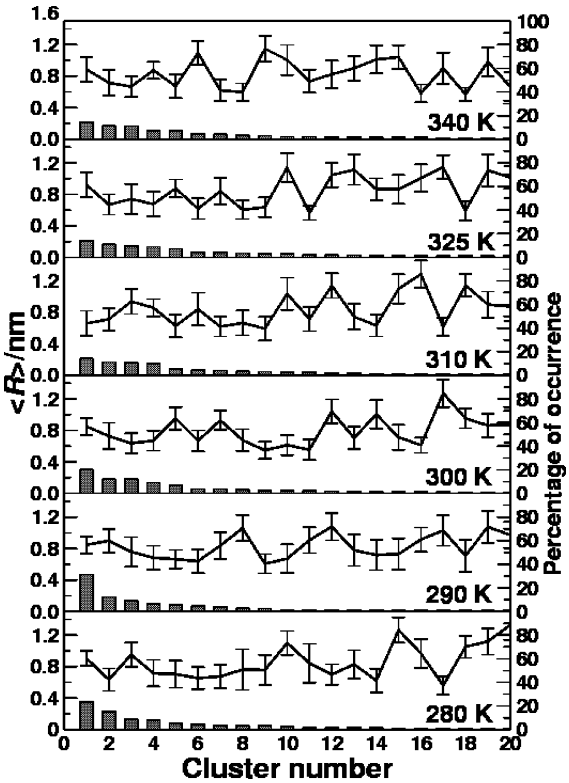

Figure 3. Average end-to-end distance for the first 20 clusters from the cumulative simulations at different temperatures. The histograms indicate the percentage of the analyzed configurations belonging to each cluster.

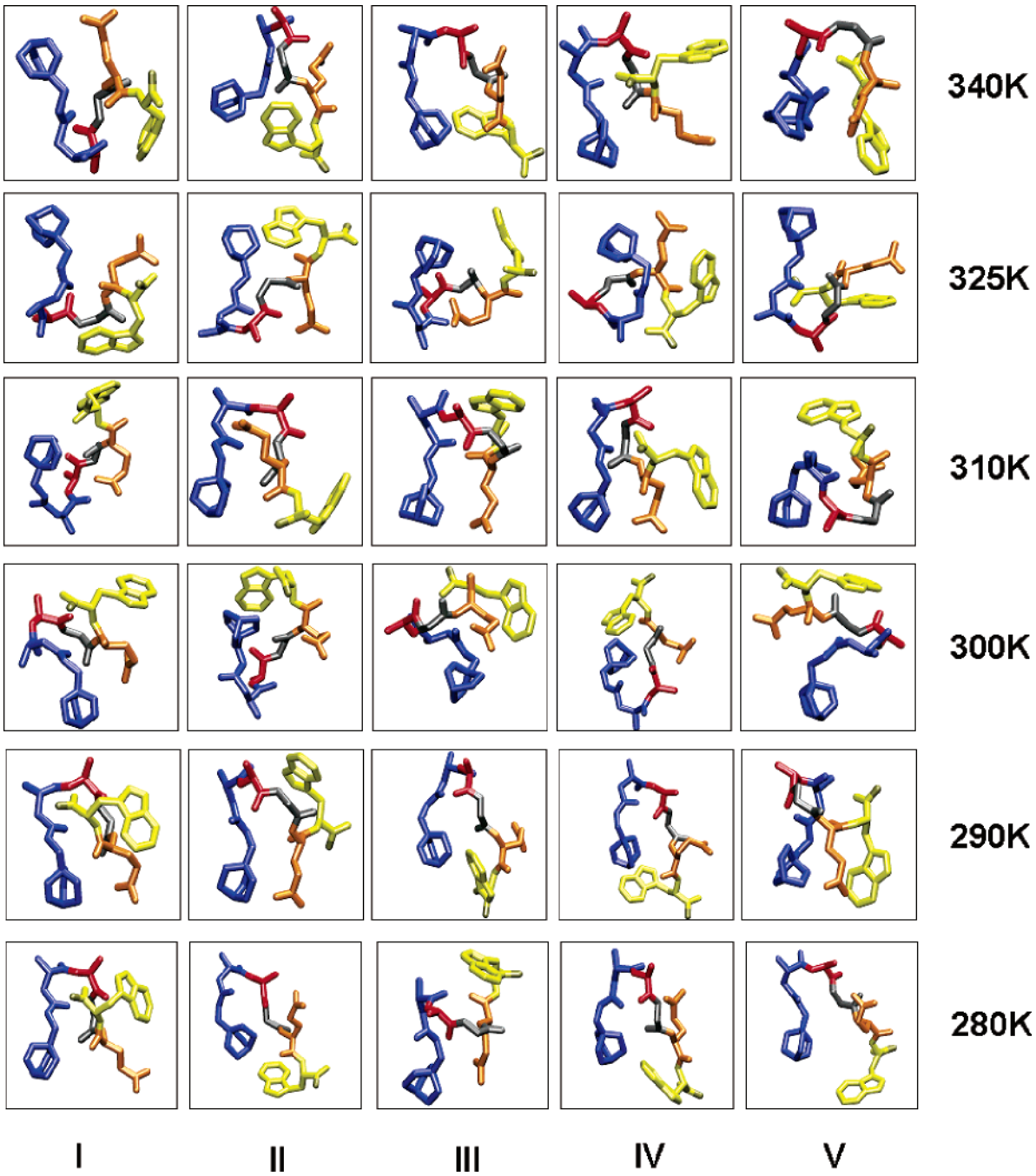

Figure 4. Representative conformations of the first 5 most populated clusters from the cumulative simulations at different temperatures. The colors differentiate the 5 different amino acids.

in Table 3), as expected for a systematic variation. The difficulties of simple force fields to reproduce experimental peptide dynamics has been addressed previously; in the case of the GROMOS96 force field, in particular, the united atom approach may lead to an increased dynamic flexibility of computed peptides.[15] In contrast, the looping rates previously derived,[16] after corrections, from the AMBER (1.4×10^7 s^{-1}) and CHARMM (7.9×10^6 s^{-1}) force fields for the Cys-AlaGlyGln-Trp peptide appear to be somewhat too slow in comparison with the experimental and theoretical data in Table 3. Presumably, the low values can be traced back to an overestimation of the corrections due to non-diffusion-controlled quenching (17−28),[16] because experimental data suggest a much smaller correction factor on the order of 2.[1,2,4] The large variations in the presumed correction factors for the Cys/Trp probe/quencher pair (2−28) further illustrate the importance of selecting intramolecularly diffusion-controlled probe/quencher pairs like Dbo/Trp to assess looping kinetics correctly.

The systematic deviation is also reflected in the Arrhenius plots constructed from the experimental and calculated data (Figure 5), specifically in the large offset of the preexponential factors, i.e., $\ln(A/s^{-1}) = 29.4 \pm 0.1$ calculated *versus* $\ln(A) = 26.8 \pm 0.2$ experimentally determined in H_2O. In contrast, the computed activation energy ($E_a = 24.7 \pm 1.5$ kJ/mol, obtained by linear fitting) is very similar to the experimental value in H_2O (21.5 ± 1.0 kJ/mol). By omitting the calculated data point at 280 K (where conformational sampling at the fixed 100 ns simulations times may still have been insufficient), the (truncated) linear fitting provides even a better agreement with $E_a = 22.8 \pm 1.2$ kJ/mol and $\ln(A/s^{-1}) = 28.4 \pm 0.5$. Differences

TABLE 3: Comparison of the Experimental and MD-Simulated (GROMOS96 Force Field) Looping Rate Constants

T/K	$k_{loop}/(10^7\ s^{-1})^a$	$k^{MD}/(10^7\ s^{-1})$	$k_{loop}^{MD}/(10^7\ s^{-1})^b$	k_{loop}^{MD}/k_{loop}
280	4.3	29.8	14.9	3.5
290	5.8	42.6	21.3	3.6
		[71],[c] [63][d]	[25],[c] [22][d]	[4.3],[c] [3.8][d]
300	7.9	67.6	33.8	4.3
310	10.4	97.1	48.5	4.7
325	15.3	144.9	72.5	4.7
340	21.7	163.9	82.0	3.8

[a] From Table 1; the experimental values available at the next closest temperature (±3 K) were selected for comparison. [b] Corrected for the underestimated viscosity of the water solvent model; a factor of 2.0 was used for GROMOS96, this work, and a factor of 2.87 was used for AMBER and CHARMM, cf. ref 16. [c] Value for AMBER force field for Cys-AlaGlyGln-Trp peptide from ref 16. [d] Value for CHARMM force field for Cys-AlaGlyGln-Trp peptide from ref 16.

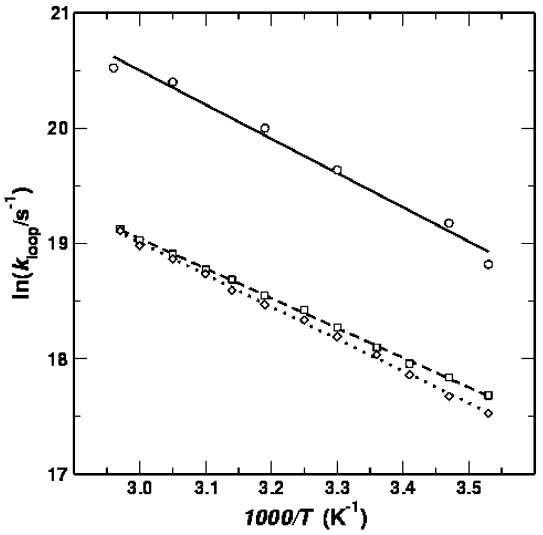

Figure 5. Arrhenius plots for the experimental (diamonds for D_2O, squares for H_2O) and MD-calculated (circles) looping rate constants and linear regression lines.

in conformational sampling may also be responsible for the fact that the MD-simulated data give rise to a slight negative curvature interpolated from the data points (Figure 5).

The good agreement of the theoretical and experimental activation energies suggests that the conformational ensembles obtained from the simulations at different temperatures represent the thermally activated looping process in a reasonable manner. Important to note, the MD-calculated activation energy is significantly higher than the activation energy anticipated from the temperature-dependent viscosity change of the water solvent model ($E_\eta = 5 \pm 1$ kJ/mol).[40] The MD-calculated looping rates in the investigated peptide are therefore not limited by solvent friction (diffusion of the chain ends by viscous flow through the solvent medium), but rather by an internal friction (barriers toward conformational changes as imposed by the stiffness of the peptide backbone). The experimental data do in fact signal a sizable contribution of internal friction as well, because the experimental activation energy for looping in water (21.5 ± 1.0 kJ mol^{-1}) lies significantly above the values expected for viscous flow of water (15.5 kJ mol^{-1}),[11] and also above those measured for more flexible Gly-Ser repeat peptides.[12] Similar conclusions were recently drawn by Buscaglia et al., who reinvestigated the Cys-AlaGlyGln-Trp peptide and its longer homologues in highly denaturing and more viscous solvents.[3] Short peptides such as the one investigated herein do in general display larger deviations from ideal-chain behavior than longer ones do.[10−12,34] In particular, they show a higher internal friction, which results in lower diffusion coefficients of the chain ends and larger activation energies for looping.[12,34] This is due to the limited conformational freedom of short peptides, which reduces the number of low-energy conformations suitable to induce quenching.

Conclusions

The combination of nanosecond time-resolved optical spectroscopy and long time-scale MD simulations allows an improved understanding of the time scale and atomistic details of intrachain motions in peptides. The direct comparison of absolute looping rate constants is difficult, however, because they depend on the choice of the experimental model, in particular on the choice of the probe/quencher pair and on the choice of the force field. As demonstrated herein, the Dbo/Trp pair affords experimental looping rates that are more than 5 times faster than those previously derived from the Trp/Cys probe/quencher pair. Similarly, the choice of the GROMOS96 force field in MD simulations affords looping rates that are faster than those obtained by several alternative force fields, which renders a universal "calibration" of MD methods virtually impossible. We have therefore resorted to the analysis of relative trends in the calculated rate constants and observed an excellent agreement when temperature-dependent rate constants and the related activation energies were investigated. MD simulations may consequently constitute an ideal tool to separate internal from solvent friction in peptide motions, which is experimentally difficult to evaluate. In addition, regardless of the deficiencies of the absolute rate constants, MD simulations with "kinetically fast" force fields like GROMOS96 have the advantage that long time-scale processes such as protein folding can become accessible at a lower computational cost but with satisfactory accuracy as far as the activation barriers for different processes and therefore the folding mechanisms may be concerned.

With respect to the implications of our study for protein folding,[41−47] its initial steps are generally thought to be due to mutual diffusive motions of chain segments, i.e., "diffusion-controlled" intrachain collisions. The end-to-end collision rates assessed by the Dbo/Trp fluorescence probe/quencher pair,[9−13] as well as by alternative triplet probe/quencher pairs[1−8] allow the direct experimental measurement of the respective intrachain motions. The temperature dependence investigated herein through a combination of experiment and MD calculations, along with previous experimental indications,[3,11,12,46] suggest that intrachain collisions in peptide segments are not fully diffusion-controlled in the sense that the rate is solely limited by solvent friction (as commonly conceptualized for bimolecular reactions), but that they are strongly modulated by internal friction. This means that the "diffusion-limited" rate and associated activation energy of any initial protein folding step depends strongly on the amino acid sequence, which constitutes a strong motivation for more comprehensive investigations on the intrachain collision kinetics of different peptides.

Acknowledgment. This study was performed using the computational resources of the CLAMV (Computer Laboratories for Animation, Modeling, and Visualization) within the graduate program "Nanomolecular Science" at Jacobs University Bremen.

Supporting Information Available: Details on the MD simulations, the parametrization of the synthetic amino acid Dbo,

and tabulated rate data in D_2O as solvent. This material is available free of charge via the Internet at http://pubs.acs.org.

References and Notes

(1) Lapidus, L. J.; Eaton, W. A.; Hofrichter, J. *Proc. Natl. Acad. Sci. U.S.A.* **2000**, *97*, 7220.

(2) Lapidus, L. J.; Steinbach, P. J.; Eaton, W. A.; Szabo, A.; Hofrichter, J. *J. Phys. Chem. B* **2002**, *106*, 11628.

(3) Buscaglia, M.; Lapidus, L. J.; Eaton, W. A.; Hofrichter, J. *Biophys. J.* **2006**, *91*, 276.

(4) Lapidus, L. J.; Eaton, W. A.; Hofrichter, J. *Phys. Rev. Lett.* **2001**, *87*, 2581011.

(5) Kubelka, J.; Hofrichter, J.; Eaton, W. A. *Curr. Opin. Struct. Biol.* **2004**, *14*, 76.

(6) Bieri, O.; Wirz, J.; Hellrung, B.; Schutkowski, M.; Drewello, M.; Kiefhaber, T. *Proc. Natl. Acad. Sci. U.S.A.* **1999**, *96*, 9597.

(7) Krieger, F.; Fierz, B.; Bieri, O.; Drewello, M.; Kiefhaber, T. *J. Mol. Biol.* **2003**, *332*, 265.

(8) Krieger, F.; Moglich, A.; Kiefhaber, T. *J. Am. Chem. Soc.* **2005**, *127*, 3346.

(9) Huang, F.; Nau, W. M. *Angew. Chem. Int. Ed.* **2003**, *42*, 2269.

(10) Hudgins, R. R.; Huang, F.; Gramlich, G.; Nau, W. M. *J. Am. Chem. Soc.* **2002**, *124*, 556.

(11) Huang, F.; Hudgins, R. R.; Nau, W. M. *J. Am. Chem. Soc.* **2004**, *126*, 16665.

(12) Sahoo, H.; Hennig, A.; Nau, W. M. *Int. J. Photoenergy* **2006**, DOI 10.1155/IJP/2006/89638.

(13) Huang, F.; Nau, W. M. *Res. Chem. Intermed.* **2005**, *31*, 717.

(14) Neuweiler, H.; Schulz, A.; Bohmer, M.; Enderlein, J.; Sauer, M. *J. Am. Chem. Soc.* **2003**, *125*, 5324.

(15) Roccatano, D.; Nau, W. M.; Zacharias, M. *J. Phys. Chem. B* **2004**, *108*, 18734.

(16) Yeh, I.-C.; Hummer, G. *J. Am. Chem. Soc.* **2002**, *124*, 6563.

(17) Smith, P. E.; van Gunsteren, W. F. *Chem. Phys. Lett.* **1993**, *215*, 315.

(18) van Gunsteren, W. F.; Billeter, S. R.; Eising, A. A.; Hünenberger, P. H.; Krüger, P.; Mark, A. E.; Scott, W. R. P.; Tironi, I. G. *Biomolecular Simulation: The GROMOS96 Manual and User Guide*; vdf Hochschulverlang: Zürich, Switzerland, 1996.

(19) Breneman, C. M.; Wiberg, K. B. *J. Comput. Chem.* **1990**, *11*, 361.

(20) Frisch, M. J.; Trucks, G. W.; Schlegel, H. B.; Scuseria, G. E.; Robb, M. A.; Cheeseman, J. R.; Montgomery, J.; J. A.; Vreven, T.; Kudin, K. N.; Burant, J. C.; Millam, J. M.; Iyengar, S. S.; Tomasi, J.; Barone, V.; Mennucci, B.; Cossi, M.; Scalmani, G.; Rega, N.; Petersson, H.; Hada, M.; Ehara, M.; Toyota, K.; Fukuda, R.; Hasegawa, J.; Ishida, M.; Nakajima, T.; Honda, Y.; Kitao, O.; Nakai, H.; Klene, M.; Li, X.; Knox, J. E.; Hratchian, H. P.; Cross, J. B.; Bakken, V.; Adamo, C.; Jaramillo, J.; Gomperts, R.; Stratmann, R. E.; Yazyev, O.; Austin, A. J.; Cammi, R.; Pomelli, C.; Ochterski, J. W.; Ayala, P. Y.; Morokuma, K.; Voth, G. A.; Salvador, P.; Dannenberg, J. J.; Zakrzewski, V. G.; Dapprich, S.; Daniels, A. D.; Strain, M. C.; Farkas, O.; Malick, D. K.; Rabuck, A. D.; Raghavachari, K.; Foresman, J. B.; Ortiz, J. V.; Cui, Q.; Baboul, A. G.; Clifford, S.; Cioslowski, J.; Stefanov, B. B.; Liu, G.; Liashenko, A.; Piskorz, P.; Komaromi, I.; Martin, R. L.; Fox, D. J.; Keith, T.; Al-Laham, M. A.; Peng, C. Y.; Nanayakkara, A.; Challacombe, M.; Gill, P. M. W.; Johnson, B.; Chen, W.; Wong, M. W.; Gonzalez, C.; Pople, J. A. *Gaussian 03*, revision B.01; Gaussian, Inc.: Wallingford, CT, 2004.

(21) Sinicropi, A.; Pischel, U.; Basosi, R.; Nau, W. M.; Olivucci, M. *Angew. Chem. Int. Ed.* **2000**, *39*, 4582.

(22) Jorgensen, W. L. *Encyclopedia of Computational Chemistry*; Wiley: New York, 1998.

(23) Jorgensen, W. L.; Tirado-Rives, J. *J. Am. Chem. Soc.* **1988**, *110*, 1657.

(24) Berendsen, H. J. C.; van der Spoel, D.; van Drunen, R. *Comput. Phys. Commun.* **1995**, *13*, 43.

(25) Lindahl, E.; Hess, B.; van der Spoel, D. *J. Mol. Model.* **2001**, *7*, 306.

(26) Hess, B. *J. Chem. Phys.* **2002**, *116*, 209.

(27) Daura, X.; Jaun, B.; Seebach, D.; van Gunsteren, W. F.; Mark, A. E. *J. Mol. Biol.* **1998**, *280*, 925.

(28) Smith, L. J.; Daura, X.; van Gunsteren, W. F. *Proteins: Struct., Funct., Genet.* **2002**, *48*, 487.

(29) Sahoo, H.; Roccatano, D.; Zacharias, M.; Nau, W. M. *J. Am. Chem. Soc.* **2006**, *128*, 8118.

(30) Lapidus, L. J.; Eaton, W. A.; Hofrichter, J. *J. Mol. Biol.* **2002**, *319*, 19.

(31) Portman, J. J. *J. Chem. Phys.* **2003**, *118*, 2381.

(32) Cornell, W. D.; Cieplak, P.; Bayly, C. I.; Gould, I. R.; Merz, K. M.; Ferguson, D. M.; Spellmeyer, D. C.; Fox, T.; Caldwell, J. W.; Collman, P. A. *J. Am. Chem. Soc.* **1995**, *117*, 5179.

(33) Brooks, B. R.; Bruccoleri, R. E.; Olafson, D. B.; States, D. J.; Swaminathan, S.; Karplus, M. J. *J. Comput. Chem.* **1983**, *4*, 187.

(34) Wang, X.; Bodunov, E. N.; Nau, W. M. *Opt. Spectrosc.* **2003**, *25*, 560.

(35) Nau, W. M.; Greiner, G.; Rau, H.; Olivucci, M.; Robb, M. A. *Ber. Bunsen−Ges.* **1998**, *102*, 486.

(36) The error of this rate constant, estimated from the error bars in the graphical representation of the scaled rate data (value for $n = 4$ in Figure 3 of ref 1), is ca. 10%.

(37) Daidone, F. S.; Roccatano, D.; Broglia, R. A.; Tiana, G.; Colombo, G.; DiNola, A. *Proteins: Struct., Funct., Bioinf.* **2004**, *57*, 198.

(38) van Gunsteren, W. F.; Bakowies, D.; Baron, R.; Chandrasekhar, I.; Christen, M.; Daura, X.; Gee, P.; Geerke, D. P.; Glättli, A.; Hünenberger, P. H.; Kastenholz, M. A.; Oostenbrink, C.; Schenk, M.; Trzesniak, D.; van der Vegt, N. F. A.; Yu, H. B. *Angew. Chem. Int. Ed.* **2006**, *45*, 4064.

(39) Klapstein, D.; Pischel, U.; Nau, W. M. *J. Am. Chem. Soc.* **2002**, *124*, 11349.

(40) To obtain the apparent activation energy for solvent viscous flow (E_η), the viscosity of the SPC water model was evaluated at different temperatures by using the method described by Hess (ref 26). The viscosities (in cP) obtained from the simulations were 0.60 at 280 K, 0.42 at 300 K, and 0.26 at 340 K, which afforded $E_\eta = 5 \pm 1$ KJ mol^{-1} ($r = 0.975$, $n = 3$).

(41) Hagen, S. J.; Hofrichter, J.; Szabo, A.; Eaton, W. A. *Proc. Natl. Acad. Sci. U.S.A.* **1996**, *93*, 11615.

(42) Munoz, V.; Thompson, P. A.; Hofrichter, J.; Eaton, W. A. *Nature* **1997**, *390*, 196.

(43) Eaton, W. A.; Munoz, V.; Thompson, P. A.; Henry, E. R.; Hofrichter, J. *Acc. Chem. Res.* **1998**, *31*, 745.

(44) Gruebele, M. *Annu. Rev. Phys. Chem.* **1999**, *50*, 485.

(45) Eaton, W. A.; Munoz, V.; Hagen, S. J.; Jas, G. S.; Lapidus, L. J.; Henry, E. R.; Hofrichter, J. *Annu. Rev. Biophys. Biomol. Struct.* **2000**, *29*, 327.

(46) Hagen, S. J.; Carswell, C. W.; Sjolander, E. M. *J. Mol. Biol.* **2001**, *305*, 1161.

(47) Sadqi, M.; Fushman, D.; Munoz, V. *Nature* **2006**, *442*, 317.